Biochemical and Biophysical Research Communications 439 (2013) 459–463

Contents lists available at ScienceDirect

Biochemical and Biophysical Research Communications

journal homepage: www.elsevier.com/locate/ybbrc

Rhodamine-based "turn-on" fluorescent probe with high selectivity for Fe^{2+} imaging in living cells

Gui-Ge Hou *, Chun-Hua Wang, Ju-Feng Sun, Mei-Zi Yang, Dong Lin, Hong-Juan Li

School of Pharmacy, Binzhou Medical University, Yantai 264003, PR China

ARTICLE INFO

Article history:
Received 24 August 2013
Available online 8 September 2013

Keywords:
Rhodamine
Fluorescent probe
Fe^{2+} ion
High selectivity
Confocal laser scanning microscopy

ABSTRACT

A rhodamine-based "turn-on" fluorescent probe **1** was synthesized with high yield. The recognizing behavior displays high selectivity of **1** toward Fe^{2+} with a 2:1 complex, and **1** exhibits a stable response for Fe^{2+} over a concentration range from 2 μM to 24 μM. Most importantly, probe is hardly interfered by other transition metal ions. Their fluorescent enhancement is observed in the presence of Fe^{2+} because of the ring-open interactions of spirocyclic. All measurements are made in PBS buffer environments simulating biological conditions to make them suitable candidates for fluorescent labeling of biological systems. Confocal laser scanning microscopy experiments have proven that probe can be used to monitor Fe^{2+} in living cells.

1. Introduction

Detection of trace amounts of iron has received increasing attention due to their vital role in biological and environmental processes [1–4]. The biological functions of iron are based on it favorable redox potential, which allows this metal to undergo interconversion between the divalent cationic or ferrous (Fe^{2+}) and trivalent cationic or ferric (Fe^{3+}) states in many biochemical processes [5]. Disorder of iron content within the body has been associated with increasing incidence of some dysfunction, such as metabolism cause anemia, liver and kidney damage, diabetes, heart failure and neurodegenerative diseases [5–7]. Therefore, a convenient and rapid method for the analysis of Fe^{2+} and Fe^{3+} in biological samples has important consequences in biological concerns. During past decades, some successful attempts have been made to develop selective fluorescent probes for Fe^{3+} [8–18]. Unfortunately, there have been relatively few fluorescent probes for Fe^{2+} [19–23]. Therefore, the development of new iron fluorescent probes with high selectivity and sensitivity for Fe^{2+} is still a great challenge as well as more interest.

On the other hand, rhodamine-based fluorescent probes with the construction of a "turn-on" type have received increasing interest in recent years because of their simplicity, low detection limit, the capability for special recognition and excellent spectroscopic properties [24–27]. Many derivatives of rhodamine undergo equilibrium between spirocyclic and ring-open forms, corresponding to the nonfluorescent formation ("off" signal) and the strongly fluorescent formation ("on" signal), respectively. In the "turn-on" process, some crucial factors maybe influence the switching degree of probes, such as protons and metal ions (Hg^{2+}, Zn^{2+}, Fe^{3+}, Cu^{2+}, etc), which can bind probe resulting in a ring-opened form with fluorescence enhancement (550–600 nm). The fluorescence-enhancement probes can efficiently overcome some disadvantages, such as relatively high background interference and lower sensitivity. So far, the lack of suitable fluorescent iron indicators is even more evident when judged in terms of application-oriented features. Some receptors employed are often selected to simulate the mechanism of ferrichromes or siderophores, however, the indication is mostly signaled by fluorescence quenching due to the paramagnetic nature of ionic iron [10,28]. Optical cellular imaging with fluorescence-enhancement probes might be the best choice for visualizing the intracellular iron by virtue of its high sensitivity, high-speed spatial analysis, and less cell-damaging [29]. It would be best that the probes employed can pass through the cell membranes to display a rapid and reversible fluorescence enhancement response in the visible range or lower energy with high selectivity for target iron over other biologically abundant cations. However, many iron fluorescent probes reported in the literature were based on fluorescence quenching mechanism [21,28,30], which were not appropriate for fluorescence imaging of target iron in living cells. Rhodamine-based fluorescent probes based on fluorescence-enhancement can theoretically avoid most of the problems for above-mentioned advantages. So the rhodamine-based framework is an ideal model to construct the "turn-on" fluorescent probes.

In this paper, 2,6-diacetylpyridine is selected to synthesize a rhodamine-based fluorescent probe **1** with high selectivity for Fe^{2+} (Scheme 1).

* Corresponding author.
E-mail address: guigehou@163.com (G.-G. Hou).

0006-291X/$ - see front matter © 2013 Elsevier Inc. All rights reserved.
http://dx.doi.org/10.1016/j.bbrc.2013.08.092

2. Experimental

2.1. Materials

Rhodamine 6G, 2,6-diacetylpyridine were purchased from Alfa Aesar. All the other chemicals (Acros) were used as obtained without further purification. RAW 264.7 cells were purchased from American Type Culture Collection, Manassas.

2.2. Methods

The stock solution of **1** (0.1 mM) was prepared in 50% MeOH, 50% H_2O. All metal ions were prepared as 0.1 mM in water. The Fe^{2+} solution was prepared immediately before use with ferrous ammonium sulfate. The solutions of Fe^{3+}, Al^{3+}, Mg^{2+}, Ca^{2+}, Cr^{3+} were performed from their chloride salts. The solutions of Co^{2+}, Ni^{2+}, Cu^{2+}, Zn^{2+}, Hg^{2+}, Mn^{2+} and Pb^{2+} were prepared from the perchlorates. Different concentrations of metal ions were added to PBS buffer (2.0 mL, 0.1 M, pH = 7.4) and **1** (1.0 mL, 0.1 mM) in a 10 mL color comparison tube. After dilution with doubly distilled water, the mixture was equilibrated for 10 min before measurement. The excitation was performed at 510 nm for all the emission studies. All fluorescence measurements were carried out on a WGY-10 Spectrofluorimeter equipped with a xenon lamp and 1.0 cm quartz carrier at room temperature. Infrared (IR) samples were prepared as KBr pellets, and spectra were obtained in the 400–4000 cm^{-1} range using a Perkin–Elmer 1600 FTIR spectrometer. Elemental analyses were performed on a Perkin–Elmer Model 2400 analyzer. ^1H NMR data were collected using an AM-400 spectrometer. Chemical shifts are reported in δ relative to TMS. The images were taken using a TCS confocal laser scanning microscope (Germany Leica Co., Ltd) with an objective lens (×40). The excitation wavelength was 532 nm.

2.3. Preparation *1*

2,6-Diacetylpyridine (0.50 g, 3.0 mmol) and **2** [24] (1.24 g, 3.0 mmol) were mixed in boiling methanol with 3 drops of formic acid. The mixture was stirred for 3 h at 70 °C (monitored by TLC). After removal of solvent under vacuum, the residue was purified on silica gel by column using CH_2Cl_2/MeOH (30:1, v/v) as the eluent to afford **1** as the white solids (1.40 g). Yield: 84%. M. p. = 254–256 °C, IR(KBr pellet cm^{-1}): 3384(s), 2966(m), 2924(m), 2856(m), 1685(s), 1622(s), 1512(s), 1417(s), 1361(s), 1271(s), 1200(s), 1161(m), 1007(m), 862(m), 818(m), 739(m). ^1H NMR (400 MHz, DMSO) δ 7.96 (d, J = 1.9 Hz, 2H), 7.89 (dd, J = 5.7, 2.7 Hz, 1H), 7.76 (dd, J = 7.1, 2.0 Hz, 1H), 7.59 (s, 2H), 7.10 (dd, J = 5.7, 2.5 Hz, 1H), 6.26 (d, J = 15.9 Hz, 4H), 5.04 (s, 2H), 3.11 (dd, J = 7.0, 5.6 Hz, 4H), 2.65 (s, 3H), 2.35 (s, 3H), 1.89 (s, 6H), 1.20 (t, J = 7.1 Hz, 6H). Anal. Calcd. for $C_{35}H_{35}N_5O_3$: C 75.37, H 6.32, N 12.55; Found: C 75.12, H 6.41, N 12.68.

2.4. Cell incubation and imaging

RAW 264.7 macrophages were cultured in Dulbecco's modified Eagle's medium containing 10% fetal bovine serum, 1% penicillin, and 1% streptomycin at 37 °C in a 5% CO_2/95% air incubator MCO-15AC (SANYO). The concentration of counted cells was adjusted to 1.0×10^6 cells mL^{-1} and cells were passed and plated on glass slide at 37 °C, 5% CO_2 for 4 h. Some of adherent cells were incubated with 20 μM probe for 0.5 h at 37 °C under 5% CO_2 and then washed with phosphate-buffered saline (PBS) three times before incubating with 20 μM $FeSO_4$ for another 0.5 h, cells were rinsed with PBS three times again, then the fluorescence imaging of intracellular Fe^{2+} was observed under a Leica TCS confocal laser scanning microscope with an objective lens (40×). The RAW 264.7 macrophages only incubated with 20 μM probe for 0.5 h at 37 °C under 5% CO_2 was as a control.

3. Results and discussion

3.1. Structural analysis

Probe **1** was synthesized in high yield by refluxing **2** with 2,6-diacetylpyridine in methanol (Scheme 1). The structure has been confirmed using ^1H NMR, IR, ESI-MS and elemental analysis. All the spectroscopic studies were performed in 20 mM PBS buffer system (pH 7.4). Probe **1** was colorless powder and found to be very stable in the above-mentioned solution system for more than 1 week.

3.2. Selectivity analysis

We investigated the spectral properties under simulated physiological conditions (20 mM PBS buffer, pH 7.4). Probe **1** exhibits an emission maximum at 562 nm. The addition of 50 μM (10 equiv.) Fe^{2+} immediately yields a pink solution with a strong fluorescence signal at 571 nm. There is 60-fold fluorescent enhancement for 1 with Fe^{2+} (Fig. 1A), which can be ascribed to the delocalized xanthene moiety of the rhodamine group [31]. However, the fluorescence spectra of 1 (5 μM) with an addition of other cations (50 μM), such as Mg^{+}, Ca^{2+}, Co^{2+}, Cr^{3+}, Cu^{2+}, Fe^{3+}, Mn^{2+}, Ni^{2+}, Pb^{2+}, Al^{3+} or Zn^{2+}, exhibits relatively weak changes in fluorescence intensity (Fig. 1A). Only added Hg^{2+}, **1** shows slight fluorescent enhancement (18-fold), which was probably the emission of trace open-ring molecules of **1**. The results show the high selectivity of **1** toward Fe^{2+} over other metal ions, which is further discussed below.

To assess the selectivity of the method, the effect of other metal ions on the determination of 50 μM Fe^{2+} was examined individually. Under the same conditions, the fluorescence spectra of **1** (5 μM) and Fe^{2+} (50 μM) with an addition of other cations (50 μM) was investigated. The relative fluorescence intensities of **1** with various cations are shown in Fig. 1B. When Fe^{2+} existed in

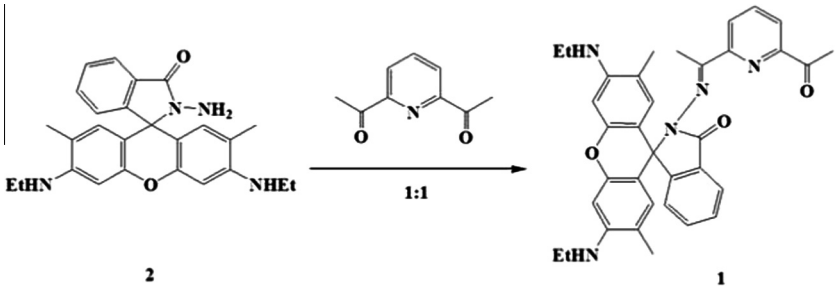

Scheme 1. Synthesis and structure of **1**.

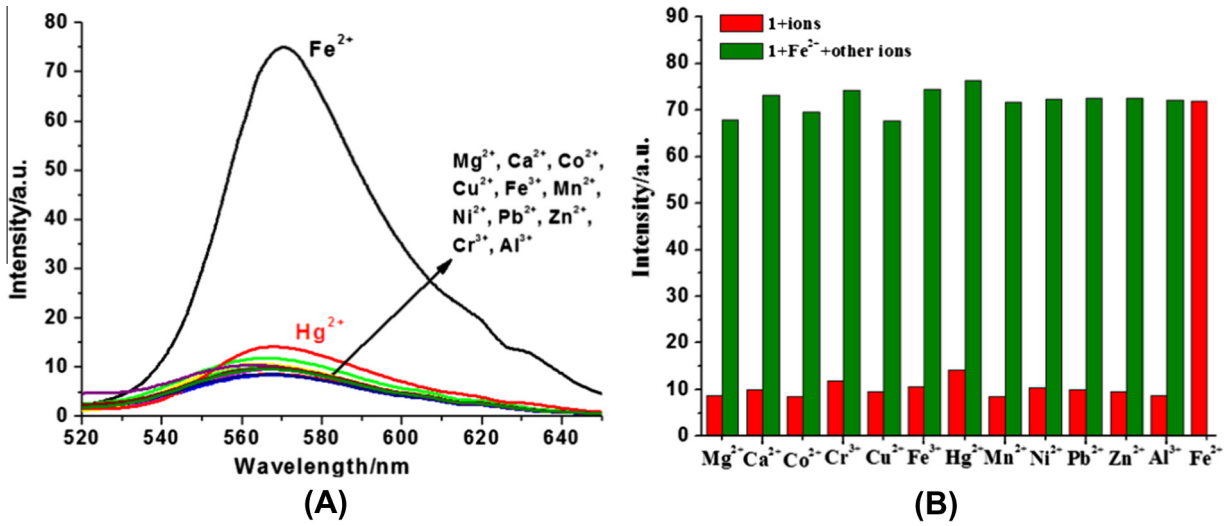

Fig. 1. (A) Fluorescence spectra of **1** (5 μM) in 20 mM PBS buffer (pH 7.4) with different metal ions (50 μM). (B) The relative fluorescence intensity of 5 μM **1** in the presence of various cations of interest in 20 mM PBS buffer (pH 7.4). Red bars: **1** with different metal ions (50 μM). Green bars: **1** and Fe^{2+} (5 μM) with an addition of other cations (50 μM). Excitation was provided at 510 nm. (For interpretation of the references to color in this figure legend, the reader is referred to the web version of this article.)

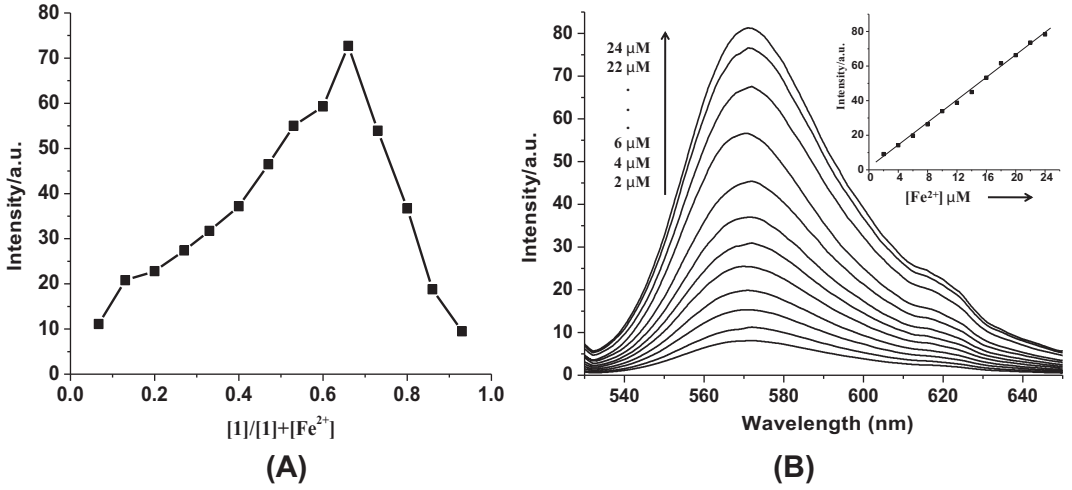

Fig. 2. (A) Job's plot of **1** with Fe^{2+} at a total concentration 30 μM. The data are consistent with a 2:1 (probe **1**:Fe^{2+}) complex. (B) Linear correlation between fluorescent intensity and Fe^{2+} concentration in the range 2–24 μM in 20 mM PBS buffer (pH 7.4).

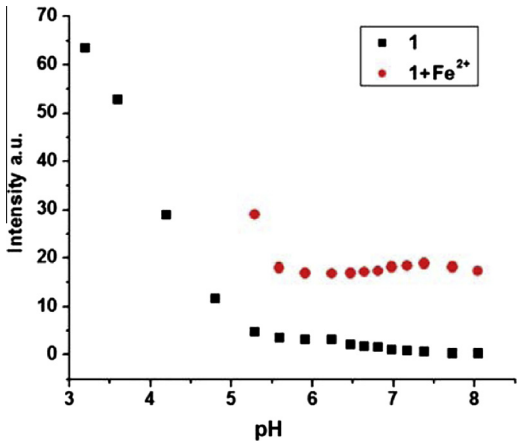

Fig. 3. The pH-controlled emission measurement of 5 μM free **1** (in 562 nm) or **1** with 50 μM Fe^{2+} (in 571 nm) at different pH conditions. Excitation was provided at 510 nm.

the solution, **1** shows few discernible fluorescent enhancements even if an addition of other cations were added. Notably, **1** is highly Fe^{2+}-selective.

Job plot analysis revealed a 2:1 complex between **1** and Fe^{2+} in solution according to the inflection point at 0.67 (Fig. 2A). Moreover, Fig. 2B and the inset indicate that there was a good linear correlation between fluorescent intensity and Fe^{2+} concentration in the range 2–24 μM ($R = 0.9983$). The regression equation was $F = 3.3364\ [Fe^{2+}]\ (\mu M) + 0.1273$.

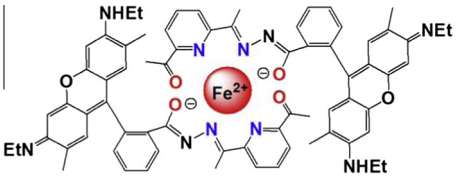

Scheme 2. The open-cycle 2:1 complex for **1** with Fe^{2+}.

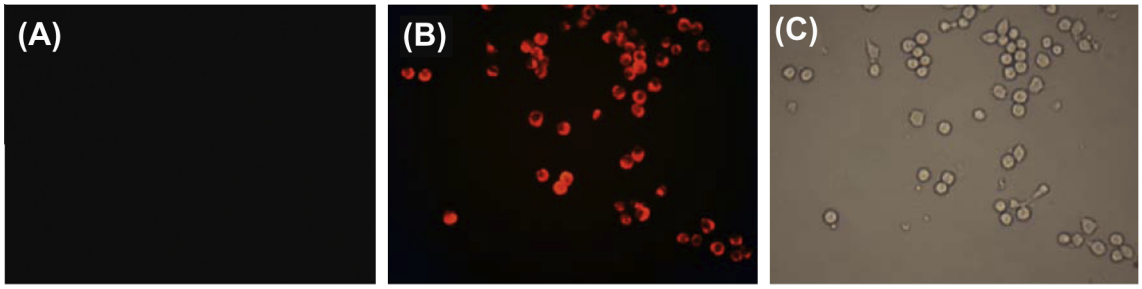

Fig. 4. Confocal fluorescence images of live RAW 264.7 macrophages. (A) Cells incubated with 20 μM probes for 30 min at 37 °C. (B) Then further incubated with 20 μM Fe^{2+} for 30 min at 37 °C. (C) Bright field image of live RAW 264.7 macrophages shown in panel, confirming their viability.

As shown in Fig. 3, the fluorescence intensity of free **1** (562 nm) in buffers of different pH was investigated. An obvious increasing color change was found along with increasing acidity (pH <5.3), which suggests the ring-open form. Even more important, probe **1** exists in the ring closed form with very weak fluorescence signal at 571 nm upon excitation at 510 nm in a wide range of pH 5.3–8.0, suggesting that the spirocyclic form was still preferred in this range. The pH-controlled emission measurement reveal that **1** can respond to iron in the pH range from 5.5 to 8.0 with the fluorescent intensity varying less than 10%, while the luminescence of free probe can be negligible. That is to say, probe works well under physiological conditions. When the pH value is lower than 5.5, the fluorescence enhancement occurs not only upon the coordination of metal ion but also with the decreasing pH values.

3.3. Mechanism analysis

The rhodamine-based complexation is an ideal model from which to construct "off-on" fluorescent chemoprobes because of its structural equilibrium between spirocyclic ("off" signal) and ring-open ("on" signal) forms. Addition of metal cation leads to a spirocycle opening via reversible coordination or irreversible chemical reaction, resulting in the appearance of pink color and orange fluorescence [24–27]. As discussed above, 2:1 complex in **1** between probes and iron are proved. It may be ascribed to the open-cycle mechanism. In Scheme 2, Fe^{2+} can bind with the amide oxygen and acetylpyridine that causes the ring-opening. Two groups of coordinated $\{O_2N_2\}$ units can satisfy the saturated coordination sphere of Fe^{2+}. The tunable luminescent property [32,33] of **1** is corresponding to luminescent "turn-on" signals based on the switching mechanism between spirocyclic and open-cycle forms.

3.4. Confocal imaging

Practical bioimaging applications of probe **1** in RAW 264.7 macrophages are developed by laser scanning confocal microscopy. Cultured RAW 264.7 macrophages are incubated with 20 μM probe **1** in culture medium for 30 min at 37 °C, and very weak intracellular fluorescence inside the living cells are observed (Fig. 4A). After further incubated with 20 μM Fe^{2+} for 30 min under the same condition, a significant increase in the fluorescence from the intracellular area can be observed (Fig. 4B). Bright-field transmission images of cells treated with the probes and Fe^{2+} confirm that cells are viable throughout the imaging experiments (Fig. 4C). The results indicate that the probe **1** can respond to the change of the concentration of Fe^{2+} in living cells.

4. Conclusions

A rhodamine-based "turn-on" fluorescent probe **1** was synthesized in high yield. Their selective experiments of various metal ions were investigated in PBS buffer (pH 7.4). The results display high selectivity of probe **1** toward Fe^{2+} with a 2:1 complex. The "turn-on" fluorescence may be ascribed to the switching mechanism between spirocyclic and open-cycle forms for the rhodamine-based probe **1**. Confocal laser scanning microscopy experiments have proven that the probe can be used to monitor Fe^{2+} in living cells. The present novel rhodamine-based probe can be further explored to obtain highly selective and sensitive probes.

Acknowledgments

We are grateful for financial support from the Foundation of Shandong Province (Nos. J11LF27, ZR2010HL065, ZR2012HM057) and the Foundation of Binzhou Medical University (Nos. BY2011-KYQD08, BY2012DKCX113).

References

[1] B. D'Autreaux, N.P. Tucker, R. Dixon, S. Spiro, A non-haem iron centre in the transcription factor N or R senses nitric oxide, Nature 437 (2005) 769–772.
[2] J.W. Lee, J.D. Helmann, The PerR transcription factor senses H_2O_2 by metal-catalysed histidine oxidation, Nature 440 (2006) 363–367.
[3] Z. Yang, M.Y. She, B. Yin, J.H. Cui, Y.Z. Zhang, W. Sun, J.L. Li, Z. Shi, Three rhodamine-based "off–on" chemosensors with high selectivity and sensitivity for Fe^{3+} imaging in living cells, J. Org. Chem. 77 (2012) 1143–1147.
[4] Y.M. Yang, Q. Zhao, W. Feng, F.Y. Li, Luminescent chemodosimeters for bioimaging, Chem. Rev. 113 (2013) 192–270.
[5] A.S. Dornelles, V.A. Garcia, M.N. de Lima, G. Vedana, L.A. Alcalde, M.R. Bogo, N. Schroeder, mRNA expression of proteins involved in iron homeostasis in brain regions is altered by age and by iron overloading in the neonatal period, Neurochem. Res. 35 (2010) 564–571.
[6] C. Brugnara, Iron deficiency and erythropoiesis: new diagnostic approaches, Clin. Chem. 49 (2003) 1573–1578.
[7] R.R. Crichton, D.T. Dexter, R.J. Ward, Metal based neurodegenerative diseases––from molecular mechanisms to therapeutic strategies, Coord. Chem. Rev. 252 (2008) 1189–1199.
[8] Y. Xiang, A. Tong, A new rhodamine-based chemosensor exhibiting selective Fe^{III}-amplified fluorescence, Org. Lett. 8 (2006) 1549–1552.
[9] A.J. Weerasinghe, C. Schmiesing, S. Varaganti, G. Ramakrishna, E. Sinn, Single- and multiphoton turn-on fluorescent Fe^{3+} sensors based on bis(rhodamine), J. Phys. Chem. B 114 (2010) 9413–9419.
[10] J.L. Bricks, A. Kovalchuk, C. Trieflinger, M. Nofz, M. Buschel, A.I. Tolmachev, J. Daub, K. Rurack, On the development of sensor molecules that display Fe^{III}-amplified fluorescence, J. Am. Chem. Soc. 127 (2005) 13522–13529.
[11] S. Ghosh, R. Chakrabarty, P.S. Mukherjee, Design, synthesis, and characterizations of a series of Pt_4 macrocycles and fluorescent sensing of $Fe^{3+}/Cu^{2+}/Ni^{2+}$ through metal coordination, Inorg. Chem. 48 (2009) 549–556.
[12] H. Weizman, O. Ardon, B. Mester, J. Libman, O. Dwir, Y. Hadar, Y. Chen, A. Shanzer, Fluorescently-labeled ferrichrome analogs as probes for receptor-mediated, microbial iron uptake, J. Am. Chem. Soc. 118 (1996) 12368–12375.
[13] J.P. Sumner, R. Kopelman, Alexa Fluor 488 as an iron sensing molecule and its application in PEBBLE nanosensors, Analyst 130 (2005) 528–533.
[14] X.B. Zhang, G. Cheng, W.J. Zhang, G. Shen, R.Q. Yu, A fluorescent chemical sensor for Fe^{3+} based on blocking of intramolecular proton transfer of a quinazolinone derivative, Talanta 71 (2007) 171–177.

[15] A.J. Weerasinghe, F.A. Abebe, E. Sinn, Rhodamine based turn-on dual sensor for Fe^{3+} and Cu^{2+}, Tetrahedron Lett. 52 (2011) 5648–5651.
[16] M. Zheng, H.Q. Tan, Z.G. Xie, L.G. Zhang, X.B. Jing, Z.C. Sun, Fast response and high sensitivity europium metal organic framework fluorescent probe with chelating terpyridine sites for Fe^{3+}, ACS Appl. Mater. Interfaces 5 (2013) 1078–1083.
[17] S. Dang, E. Ma, Z.M. Sun, H.J. Zhang, A layer-structured Eu-MOF as a highly selective fluorescent probe for Fe^{3+} detection through a cation-exchange approach, J. Mater. Chem. 22 (2012) 16920–16926.
[18] Y.B. Wei, Z.Y. Aydin, Y. Zhang, Z.W. Liu, M.L. Guo, A turn-on fluorescent sensor for imaging labile Fe^{3+} in live neuronal cells at subcellular resolution, ChemBioChem 13 (2012) 1569–1573.
[19] P. Li, L.B. Fang, H. Zhou, W. Zhang, X. Wang, N. Li, H.B. Zhong, B. Tang, A new ratiometric fluorescent probe for detection of Fe^{2+} with high sensitivity and its intracellular imaging applications, Chem. Eur. J. 17 (2011) 10520–10523.
[20] S. Epsztejn, O. Kakhlon, H. Glickstein, W. Breuer, Z.I. Cabantchik, Fluorescence analysis of the labile iron pool of mammalian cells, Anal. Biochem. 248 (1997) 31–40.
[21] K. Zheng, C.Y. Lai, L.P. He, F. Li, Chromo-chemodosimetric detection for Fe^{2+} by Fenton reagent-induced chromophore-decolorizing of halogenated phenolsulfonphthalein derivatives, Sci. China Chem. 53 (2010) 1398–1405.
[22] R.I. Stefan, S.G. Bairu, Monocrystalline diamond paste-based electrodes and their applications for the determination of Fe(II) in vitamins, Anal. Chem. 75 (2003) 5394–5398.
[23] T. Hirayama, K. Okuda, H. Nagasawa, A highly selective turn-on fluorescent probe for iron(II) to visualize labile iron in living cells, Chem. Sci. 4 (2013) 1250–1256.
[24] W.S. Zhang, B. Tang, X. Liu, Y.Y. Liu, K.H. Xu, J.P. Ma, L.L. Tong, G.W. Yang, A highly sensitive acidic pH fluorescent probe and its application to HepG2 cells, Analyst 134 (2009) 367–371.
[25] F.B. Yu, W.S. Zhang, P. Li, Y.L. Xing, L.L. Tong, J.P. Ma, B. Tang, Cu^{2+}-selective naked-eye and fluorescent probe: its crystal structure and application in bioimaging, Analyst 134 (2009) 1826–1833.
[26] W. Huang, C.X. Song, C. He, G.J. Lv, X.Y. Hu, X. Zhu, C.Y. Duan, Recognition preference of rhodamine-thiospirolactams for mercury(II) in aqueous solution, Inorg. Chem. 48 (2009) 5061–5072.
[27] X.F. Yang, X.Q. Guo, Y.B. Zhao, Development of a novel rhodamine-type fluorescent probe to determine peroxynitrite, Talanta 57 (2002) 883–890.
[28] J.A. Ho, H.C. Chang, W.T. Su, DOPA-mediated reduction allows the facile synthesis of fluorescent gold nanoclusters for use as sensing probes for ferric ions, Anal. Chem. 84 (2012) 3246–3253.
[29] Z.X. Han, X.B. Zhang, Z. Li, Y.J. Gong, X.Y. Wu, Z. Jin, C.M. He, L.X. Jian, J. Zhang, G.L. Shen, R.Q. Yu, Efficient fluorescence resonance energy transfer-based ratiometric fluorescent cellular imaging probe for Zn^{2+} using a rhodamine spirolactam as a trigger, Anal. Chem. 82 (2010) 3108–3113.
[30] R.G. Peng, F. Wang, Y.W. Sha, Synthesis of 5-dialkyl(aryl)aminomethyl-8-hydroxyquinoline dansylates as selective fluorescent sensors for Fe^{3+}, Molecules 12 (2007) 1191–1201.
[31] N.O. Mchedlov-Petrossyan, Protolytic equilibrium in lyophilic nanosized dispersions: differentiating influence of the pseudophase and salt effects, Pure Appl. Chem. 80 (2008) 1459–1510.
[32] G.G. Hou, Y. Liu, Q.K. Liu, J.P. Ma, Y.B. Dong, NbO lattice MOFs based on octahedral M(II) and ditopic pyridyl substituted diketonate ligands: structure, encapsulation and guest-driven luminescent property, Chem. Commun. 47 (2011) 10731–10733.
[33] Y.B. Dong, P. Wang, J.P. Ma, X.X. Zhao, H.Y. Wang, B. Tang, R.Q. Huang, Coordination-driven nanosized lanthanide "molecular lantern" with tunable luminescent properties, J. Am. Chem. Soc. 129 (2007) 4872–4873.